Toxicology 500 (2023) 153672

Contents lists available at ScienceDirect

Toxicology

journal homepage: www.elsevier.com/locate/toxicol

Arsenic induces metabolome remodeling in mature human adipocytes

Marie Gasser [a,b], Sébastien Lenglet [a], Nasim Bararpour [c,d], Tatjana Sajic [a,b], Julien Vaucher [e,f], Kim Wiskott [g], Marc Augsburger [a], Tony Fracasso [g], Federica Gilardi [a,b,*], Aurélien Thomas [a,b,*]

[a] Unit of Forensic Toxicology and Chemistry, CURML, Lausanne and Geneva University Hospitals, Lausanne, Geneva, Switzerland
[b] Faculty Unit of Toxicology, CURML, Faculty of Biology and Medicine, University of Lausanne, Lausanne, Switzerland
[c] Stanford Center for Genomics and Personalized Medicine, Stanford, CA, USA
[d] Department of Genetics, Stanford University School of Medicine, Stanford, CA, USA
[e] Service of Internal Medicine, Lausanne University Hospital and University of Lausanne, Lausanne, Switzerland
[f] Service of Internal Medicine, Fribourg Hospital and University of Fribourg, Fribourg, Switzerland
[g] Unit of Forensic Medicine, CURML, Lausanne and Geneva University Hospitals, Lausanne, Geneva, Switzerland

ARTICLE INFO

Handling Editor: Dr. Mathieu Vinken

Keywords:
Arsenic
Human adipocytes
Metabolomics
Oxidative stress response
Lipid metabolism

ABSTRACT

Human lifetime exposure to arsenic through drinking water, food supply or industrial pollution leads to its accumulation in many organs such as liver, kidneys, lungs or pancreas but also adipose tissue. Recently, population-based studies revealed the association between arsenic exposure and the development of metabolic diseases such as obesity and type 2 diabetes. To shed light on the molecular bases of such association, we determined the concentration that inhibited 17% of cell viability and investigated the effects of arsenic acute exposure on adipose-derived human mesenchymal stem cells differentiated *in vitro* into mature adipocytes and treated with sodium arsenite ($NaAsO_2$, 10 nM to 10 μM). Untargeted metabolomics and gene expression analyses revealed a strong dose-dependent inhibition of lipogenesis and lipolysis induction, reducing the cellular ability to store lipids. These dysregulations were emphasized by the inhibition of the cellular response to insulin, as shown by the perturbation of several genes and metabolites involved in the mentioned biological pathways. Our study highlighted the activation of an adaptive oxidative stress response with the strong induction of metallothioneins and increased glutathione levels in response to arsenic accumulation that could exacerbate the decreased insulin sensitivity of the adipocytes. Arsenic exposure strongly affected the expression of arsenic transporters, responsible for arsenic influx and efflux, and induced a pro-inflammatory state in adipocytes by enhancing the expression of the inflammatory interleukin 6 (IL6). Collectively, our data showed that an acute exposure to low levels of arsenic concentrations alters key adipocyte functions, highlighting its contribution to the development of insulin resistance and the pathogenesis of metabolic disorders.

1. Introduction

Arsenic (As) and inorganic arsenic compounds are classified as group I carcinogens by the International Agency for Research on Cancer (IARC), with arsenite ions As^{3+} being the most toxic form of arsenic (Jomova et al., 2011). Some of the principal mechanisms related to As toxicity in humans are the induction of cytotoxicity, oxidative stress, DNA damage and epigenetic alterations (Ochoa-Martinez et al., 2019). Population is exposed to As via environmental and occupational exposures (Coelho et al., 2014), industrial contaminations (Freire et al., 2020), agricultural products and seafood consumption (Farkhondeh et al., 2019; Qin et al., 2009; Lai et al., 1993), the latter being mostly caused by As accumulation across the food chain. Due to soil and ground water contamination, one of the main routes of As ingestion is through drinking water, which leads to chronic exposure of the population and increased risk of chronic diseases (Chen et al., 2009). During long-term exposure, As accumulates primarily in liver, but also other organs such as pancreas, kidney, lungs and adipose tissue (Freire et al., 2020; Drobna

Abbreviations: AD-hMSC, adipose-derived human mesenchymal stem cell; As, arsenic; $AsGSH_3$, arsenic-tri-glutathione complex; BMI, body mass index; HESI, heated electrospray ionization; IARC, International Agency for Research on Cancer; IC50, half inhibitory concentration; ICP-MS, inductively coupled plasma system coupled to mass spectrometry; LIMMA, linear model for microarray data; MSTUS, MS total useful signal; MT, metallothionein; T2D, type 2 diabetes; UPLC-HRMS, ultrahigh pressure liquid chromatography coupled to high resolution mass spectrometry.

* Corresponding authors at: Unit of Forensic Toxicology and Chemistry, CURML, Lausanne and Geneva University Hospitals, Lausanne, Geneva, Switzerland.
E-mail addresses: federica.gilardi@chuv.ch (F. Gilardi), aurelien.thomas@chuv.ch (A. Thomas).

https://doi.org/10.1016/j.tox.2023.153672
Received 8 August 2023; Received in revised form 30 October 2023; Accepted 10 November 2023
Available online 11 November 2023

et al., 2010; Rahman et al., 2009) where it can lead to cancer development (Lai et al., 1993; Kuo et al., 2017). Moreover, it is associated with the development of various cardiovascular diseases (Farzan et al., 2017; Kuo et al., 2017; Ochoa-Martinez et al., 2019), nervous system diseases, endocrine system dysfunction (Chen et al., 2009), reproductive impairment (Qin et al., 2009) and pulmonary diseases (Farkhondeh et al., 2019). In particular, As exposure has been associated with the development of obesity, type 2 diabetes (T2D) and metabolic syndrome. Several population-based studies showed a significant association between the prevalence of T2D and As exposure (Afridi et al., 2008; Rahman et al., 1998; Grau-Perez et al., 2017; Gribble et al., 2012; Islam et al., 2012) in a dose-response relationship in various world area (Lai et al., 1993; Chen et al., 2009; Castriota et al., 2018). In addition, As is associated with decreased fasting insulin levels and has a strong effect on glucose metabolism (Rhee et al., 2013). Indeed, blood As significantly correlates with increased blood glucose level and the associated risk of impaired glucose tolerance (Ettinger et al., 2009). As concentrations are also significantly higher in hair and urine of diabetic patients (Afridi et al., 2008) and associated with smoking status, lower school education and alcohol consumption (Gribble et al., 2012; Rhee et al., 2013; Coelho et al., 2014).

Several studies have explored at molecular and cellular levels the mechanisms underlying the negative effects of As on metabolic homeostasis. Chronic exposure to As induces pancreatic beta cell dysfunction and apoptosis, which results in a reduction of glucose-stimulated insulin secretion, impaired glucose tolerance and associated hyperglycemia (Paul et al., 2008; Paul et al., 2007a; Paul et al., 2007b; Ceja-Galicia et al., 2017; Palacios et al., 2012; Diaz-Villasenor et al., 2007; Kirkley et al., 2018). Adipose tissue, another organ with a key role in maintaining glucose and lipid balance, seems also particularly sensitive to As exposure. In mice and rats chronically exposed to As through drinking water, As accumulation was associated with increased white adipose tissue (WAT) size, increased adipocyte hypertrophy, decreased levels of Perilipin 1 (PLIN1) protein leading to deficient lipid storage and accumulation of ectopic fat in muscle (Garciafigueroa et al., 2013). Consistently with the observed defects in lipid storage, As was shown to inhibit adipocyte differentiation of murine 3T3-L1 cells and human preadipocytes. As treatment during the differentiation inhibited lipid droplet accumulation and adipogenic markers, reduced insulin-stimulated glucose uptake (ISGU) and strongly promoted lipolysis, mitochondrial damage and reactive oxygen species production (Garciafigueroa et al., 2013; Calderon-DuPont et al., 2023). Overall, As effects on differentiating adipocytes could contribute in part to the development of insulin resistance. Moreover, As also impacts murine fully differentiated adipocytes. Acute exposure of 3T3-L1 adipocytes induced a significant decrease of basal and insulin-stimulated glucose uptake, likely due to As effect on the PKB/Akt-dependent mobilization of the Glucose Transporter 4 (GLUT4) that was significantly reduced (Paul et al., 2007a; Walton et al., 2004). Upon longer exposure, the decreased insulin sensitivity of 3T3-L1 adipocytes was associated with increased Nuclear Factor Erythroid 2-Related Factor 2 (NRF2) activity, increased levels of glutathione and inflammatory cytokines, and decreased levels of markers of the adipocyte functions such as the Peroxisome proliferator-activated receptor gamma isoforms 1 and 2 (*Pparg1*, *Pparg2*) and the CCAAT enhancer binding protein alpha (*Cebpa*) (Xue et al., 2011). Collectively these data suggested that the perturbation of ISGU may be due to the cellular activation of the oxidative stress response induced by As (Wang et al., 2005; Padmaja Divya et al., 2015; Cheng et al., 2011; Garciafigueroa et al., 2013; Klei et al., 2013; Yadav et al., 2013). In contrast, little is known about the mechanistic effects of As in mature human adipocytes. Importantly, murine models might be less susceptible than humans to As toxicity because mice have faster As metabolism and clearance (Ahangarpour et al., 2018). Hence, it is of great interest to address the rodent observations in human cellular models.

To investigate the effects of As on mature human adipocytes, we first determined the As concentration that inhibited 17% of the cellular viability of Adipose-Derived human Mesenchymal Stem Cells (AD-hMSCs) differentiated into mature adipocytes *in vitro*. We determined a range of concentrations from 10 nM to 10 μM and assessed the effects of As at the metabolomic, gene expression, protein and cellular levels in mature adipocytes after 48 h of exposure. Our results demonstrated that, despite the activation of an adaptive response to oxidative stress, acute As exposure was able to dysregulate lipid metabolism, As transporters and other adipocyte functions in human adipocytes.

2. Materials and methods

2.1. Cell culture

Adipose-derived human mesenchymal stem cells (AD-hMSCs, FC-0034) were purchased at Lifeline Cell Technology (Frederick, MD, USA) and are derived from human adipose tissue isolated from adult subcutaneous lipoaspirate. Cells were obtained from two independent female donors (38 and 51 years) of Caucasian origin. AD-hMSCs are selected by the manufacturer via flow cytometry to confirm the expression of multiple mesenchymal stem cell markers. AD-hMSCs can be differentiated *in vitro* into adipocytes. Cells were expanded at 37 °C and 5% CO_2 in MesenPro RS Basal Medium supplemented with MesenPro RS Growth Supplement (Gibco, Thermo Fisher Scientific, Waltham, MA, USA) and 2 mM GlutaMAX-I (Gibco), following manufacturer instructions. Cells were splitted when they reached 80% confluency and seeded into 6-, 12- and 24-well plates at 9×10^3 cells/cm^2 in complete MesenPro RS medium. At confluence, cells were induced to differentiate into adipocytes in MesenPro Basal Medium, supplemented with 10% of Fetal Bovine Serum (FBS, Biowest, Riverside, MO, USA), 2 mM GlutaMAX-I, 0.5 mM 3-isobutyl-1-methylxanthine (IBMX, Sigma-Aldrich, Saint-Louis, MO, USA), 10 μg/mL insulin (Sigma-Aldrich), 200 μM indomethacin (Sigma-Aldrich) and 10 nM dexamethasone (Sigma-Aldrich). Cells were refed every 3 – 4 days and after two weeks of differentiation, fully differentiated adipocytes were incubated with sodium arsenite ($NaAsO_2$, Sigma-Aldrich) solutions for 48 h at 37 °C and 5% CO_2. Between 1 nM and 0.5 M of $NaAsO_2$ were used in this study. $NaAsO_2$ powder was dissolved in ultra-pure water (Milli-Q) and diluted in MesenPro RS Basal Medium supplemented with 2 mM GlutaMAX-I. Each experiment described in the following sections is the result of an independent cellular differentiation process.

2.2. Cell viability assay

AD-hMSCs were differentiated into adipocytes in 24-well plates and treated with $NaAsO_2$ (1 nM to 0.5 M; well number $N = 2$ for As concentrations between 1 nM and 100 nM and between 0.05 M and 0.5 M; $N = 3$ for As concentrations between 500 nM and 0.01 M; $N = 4$ for controls) for 48 h. The Cell Proliferation Kit I (MTT) (Roche, Basel, Switzerland) was used to assess cell viability after As treatment, following manufacturer instructions. Plates were incubated at 37 °C and 5% CO_2 for 20 min with the MTT reaction mix before extraction in 300 μL of dimethyl sulfoxide (DMSO, Sigma-Aldrich). The absorbance was measured in duplicate at 540 nm in a 96-well microplate with the Infinite M Nano Reader (Tecan, Männedorf, Switzerland). The viability rate was calculated with non-linear regression to fit the Hill function. The results are the mean of three independent experiments.

2.3. Arsenic quantification in mature adipocytes

AD-hMSCs were differentiated into adipocytes in 6-well plates and treated with $NaAsO_2$ (10 nM to 10 μM, $N = 5$) for 48 h. Cells were washed with phosphate-buffer saline (PBS, Gibco). 320 μL of HNO_3 65% were added into each well to extract cell lysates.

Total arsenic concentrations were measured by inductively coupled plasma system coupled to mass spectrometry (ICP-MS, 7800 Series;

Agilent, Palo Alto, Santa Clara, CA, USA) for elementary quantification as described previously (Perrais et al., 2023). 300 μL of cell lysate were diluted with 2.7 mL of HNO_3 0.1% containing 10 ng/mL Rhodium and 10 ng/mL Indium as internal standards. In addition, each analytical batch of study samples was processed with laboratory controls, including method blanks and standard reference materials to continuously monitor method performance.

2.4. Metabolomic study

2.4.1. Cell culture and metabolite extraction

AD-hMSCs were differentiated into adipocytes in 6-well plates and treated with $NaAsO_2$ (10 nM to 10 μM, N = 5) for 48 h. Cells were washed with PBS and immediately put on dry ice. 1.5 mL of solvent mix MeOH/EtOH/H_2O 2:2:1 containing 10 ng/mL of internal standards, hydrocodone-d6 and phenobarbital-d5, were added into each well and plates were incubated at − 80 °C for 20 min. Cells were scrapped and transferred into 2 mL Eppendorf tubes on dry ice. Tubes were agitated during 5 min with metallic beads and centrifuged for 5 min at 17 G and 4 °C to pellet cellular debris. The metabolite-containing supernatants were transferred into new Eppendorf tubes on dry ice and evaporated for 4.5 h with a CentriVap Concentrator (Labconco, Kansas City, MO, USA).

2.4.2. Sample preparation

The pellets were resuspended in 100 μL of 10% MeOH and centrifuged for 5 min at 17 G at 8 °C. The resulting supernatants were divided into two fractions of 40 μL and transferred into two glass vials for injection in positive and negative modes. Quality control (QCs) samples were a pooled matrix sample generated by combining 10 μL of each experimental sample. QCs were injected 10 times across the batch.

2.4.3. Untargeted mass spectrometry analysis

Untargeted mass spectrometry analysis was performed using ultra-high performance liquid chromatography coupled to high-resolution mass spectrometry (UPLC-HRMS). A Thermo Scientific Ultimate 3000 LC system coupled to a Q Exactive Plus system interfaced with a heated electrospray ionization (HESI-II) was used for the study. Positive and negative mode analyses used mobile phases consisting of 0.1% formic acid in water (A) and 0.1% formic acid in MeOH (B). The sample injection volume was 10 μL and separation was made using a C18 column (Phenomenex Kinetex, C18 – 100 ×2.1 mm, 2.6 μm) held at 40 °C. Mobile phase B was ramped linearly from 2% to 100% over 11 min, stayed at 100% for 6 min and brought back to 2% for a 7-minute re-equilibration stage. The total analysis run was 25 min with a flow of 400 μL/min. The mass analyzer was tuned and calibrated for mass resolution and mass accuracy and the full scan range covered 70–1000 *m/z*. The ionization spray voltage was set to 3.5 and 2.5 kV respectively in positive and negative mode, the sheath gas flowrate to 50, the auxiliary gas flowrate to 13 and the sweep gas flow rate to 3 (gas flowrates are in arbitrary units). In both modes, the capillary temperature was 320 °C and the auxiliary gas heater temperature was 425 °C. The acquisition software was Xcalibur 4.3.73.11.

2.4.4. Data analysis

Raw UPLC-HRMS data were first converted to mzXML format using ProteoWizard (Chambers et al., 2012) to be processed by XCMS online software (The Scripps Research Institute, San Diego, CA, USA) for peak detection and chromatogram alignment. Missing data were estimated using the emvd function from the dbnorm R package (Bararpour et al., 2021). Preprocessed data were normalized by the MS Total Useful Signal (MSTUS) normalization method available on the NOREVA online software (Yang et al., 2020). One-way ANOVA generated a heatmap of the top 150 metabolite features significantly altered across the four concentrations of As. Linear models for Microarray data (LIMMA) using R software were applied to compare control samples versus As-treated samples at 10 μM (Ritchie et al., 2015). Differences were considered significant if the adjusted p-value (adj. p-value) was < 0.05. Significant metabolites were identified based on their mass to charge ratio and retention time using the Human Metabolome Database (HMDB). Metabolites were characterized by MS/MS to confirm their fragmentation pattern and the identification. For heatmap generation, data were clustered in R by Ward's clustering with the Euclidean distance.

2.4.5. Over-representation pathway analysis

Over-representation pathway analysis of the metabolomic data at 10 μM was performed using ConsensusPath DB software exploiting KEGG, SMPDB, Reactome, EHMN, HumanCyc, INOH and PID databases. Pathways were considered significantly enriched when the q-value was < 0.01 and when more than three significantly impacted metabolites were found in the pathway.

2.5. RNA extraction and real time quantitative PCR

AD-hMSCs were differentiated into adipocytes in 12-well plates and treated with $NaAsO_2$ for 48 h (10 nM to 10 μM, N = 6 for controls, N = 5 for As concentrations). Total RNA was isolated from controls and As-exposed cells using the Direct-zol RNA MiniPrep Kit (Zymo Research, Lucerna-Chem, Luzern, Switzerland) following manufacturer protocol. RNA concentrations were quantified using the Qubit Fluorometer (Invitrogen, Life Technologies, Carlsbad, CA, USA) following manufacturer instructions. Following manufacturer instructions, 100 ng of total RNA were used to synthesized cDNA with the iScript™ cDNA Synthesis Kit (BioRad, Hercules, CA, USA). For real-time quantitative PCR (RT-qPCR), the target genes were either amplified with the KAPA PROBE FAST qPCR Master Mix (2X) Kit (KapaBiosystems, Sigma-Aldrich; qPCR program of 2 min at 50 °C, 3 min at 95 °C, followed by 46 cycles of 15 s at 95 °C and 30 s at 60 °C), or with the KAPA SYBR FAST qPCR Master Mix (2X) Kit (KapaBiosystems; qPCR program of 10 min at 95 °C, followed by 40 cycles of 10 s at 95 °C and one minute at 60 °C, associated with a melt curve stage of 15 s at 95 °C, one minute at 60 °C and increases of 0.3 °C every 15 s to reach 95 °C). The selected primer sets used in this study are summarized in Supplementary Table 1. Results were normalized to Ribosomal Protein S13 (RPS13) as a housekeeping gene and relative expression was calculated with the $2^{-\Delta\Delta Ct}$ method.

2.6. Oil Red O staining

AD-hMSCs were differentiated into adipocytes into 24-well plates and treated with $NaAsO_2$ (10 nM to 10 μM, N = 6 for controls, N = 7 for As concentrations) for 48 h. Cells were washed with PBS and incubated in 4% formaldehyde in H_2O for 15 min at room temperature. Formaldehyde was removed and cells were incubated with 200 μL of Oil Red O working solution made of 0.5% Oil Red O solution in isopropanol (Sigma-Aldrich) and distilled H_2O at a 2:3 ratio. Cells were then washed 5 times with distilled H_2O and pictures were taken at 20 times magnification with a Nikon eclipse TS100. Dye was eluted with 100% isopropanol for 10 min at room temperature under constant agitation. Samples were transferred in a 96-well microplate and absorbance was measured at 510 nm in duplicate with an Infinite M Nano Reader (Tecan).

2.7. Western blot

AD-hMSCs were differentiated into adipocytes in 6-well plates and treated with $NaAsO_2$ (1 and 10 μM, N = 2) for 48 h in complete differentiation medium. Cells were serum- and insulin-starved overnight during the last 16 h of As treatment and stimulated with 10 nM of insulin for 15 min at the end of the treatment. Proteins were extracted on ice with 200 μL of M-PER Mammalian Protein Extraction Reagent (Thermo Fisher Scientific, Waltham, MA, USA) supplemented with Halt Protease and Phosphatase Inhibitor Cocktail (100X) (Thermo Fisher Scientific) following manufacturer instructions. Equal amounts of proteins for each

sample were used for Western blot analysis.

Protein samples were analyzed by SDS/PAGE with standard procedures (gradient 12.5% acrylamide) and electroblotted onto Protran BA85, 0.45 μm pore size nitrocellulose membrane (Whatman, Maidstone, United Kingdom) as described previously (Gasser et al., 2022). Anti-phospho-Akt (Ser473) (9271, dilution 1:1000, Cell Signaling Technology), anti-Akt (9272, dilution 1:1000, Cell Signaling Technology), anti-GAPDH (14C10, dilution 1:1000, Cell Signaling Technology) and anti-rabbit HRP (NA934V, dilution 1:30,000 for phospho-Akt and GAPDH, 1:20,000 for Akt) antibodies were used for western blot. Detection was performed with ECL Select kit (Cytiva, Amersham, Sigma-Aldrich) in the Syngene G:BOX. Images were processed using

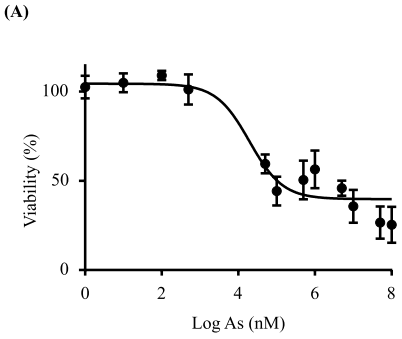

Inhibitory Concentration	Concentration (μM)
IC10	6
IC20	13
IC50	20

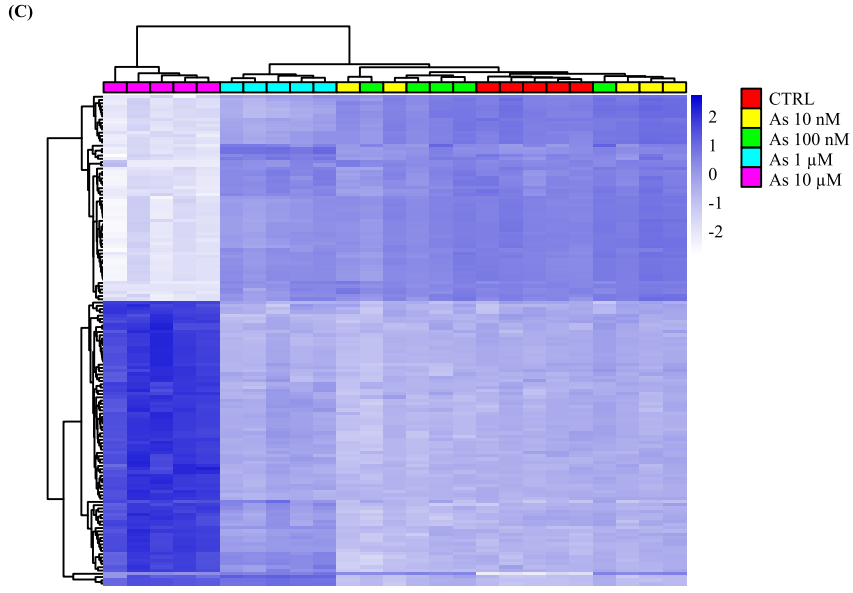

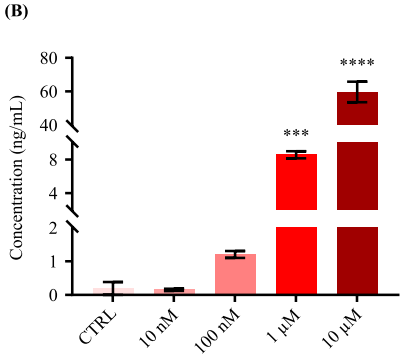

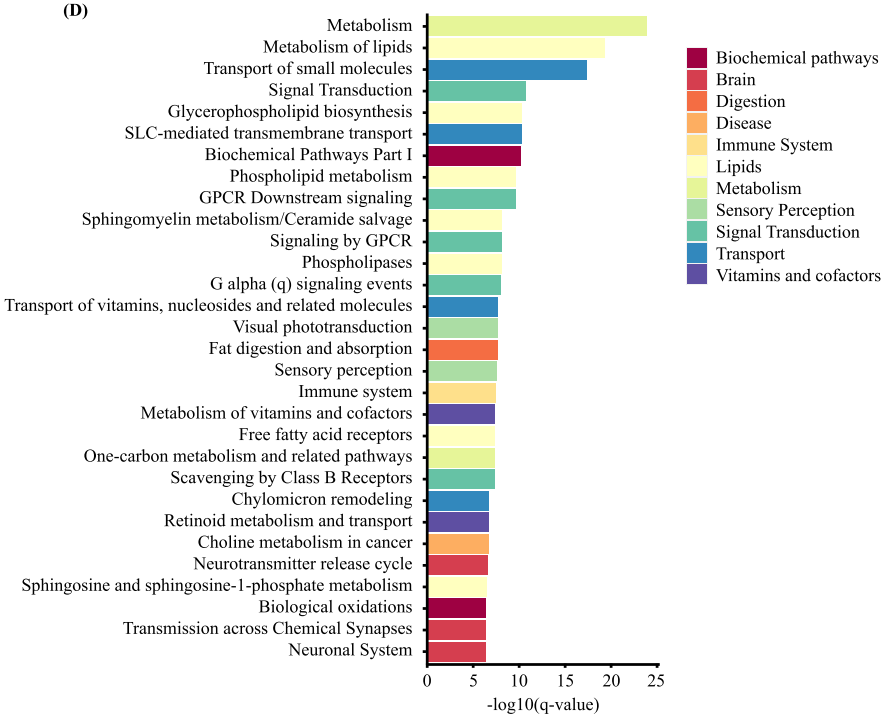

Fig. 1. Cytotoxic and metabolic impact of arsenic exposure on AD-hMSCs. (A) Determination of As cytotoxicity on AD-hMSCs treated with arsenic concentrations (1 nM – 500 mM) for 48 h. Cell viability was determined by MTT Assay and the error bars represent the standard deviation. The IC10, IC20 and IC50 were calculated using non-linear regression in GraphPad Prism and are the results of three independent experiments. (B) Arsenic concentrations were measured in cell lysates after 48 h of exposure (10 nM to 10 μM, N = 5). One-way ANOVA followed by Tukey post hoc test were used to analyze differences between controls and arsenic concentrations and * indicates significant changes versus controls (*** $p < 0.001$, **** $p < 0.0001$). The error bars represent standard deviation. (C) Representation of the 150 most significantly altered metabolite features by arsenic exposure at concentrations between 10 nM and 10 μM as revealed by one-way ANOVA. Data were clustered by Ward's clustering with the Euclidean distance in R. Heatmap columns represent controls and arsenic-treated cells (10 nM to 10 μM, N = 5) and rows represent significantly dysregulated metabolite features. (D) Over-representation pathway analysis of the 30 most significantly altered biological pathways enriched by metabolites at 10 μM of arsenic (q value < 0.01).

ImageJ software (Rasband, W.S., ImageJ, U. S. National Institutes of Health, Bethesda, MD, USA, https://imagej.nih.gov/ij/, 1997–2018). GAPDH was used as an internal loading control to confirm that protein loading was the same across the gels (Barber et al., 2005; Gorzelniak et al., 2001; Matthae et al., 2013).

2.8. Statistical analyses

One-way ANOVA followed by Tukey post hoc test were performed using GraphPad Prism version 9.1.0 (221) for Windows (GraphPad software, San Diego, CA, USA; www.graphpad.com). LIMMA analyses and heatmap generation were performed using RStudio (version 3.6.3) for Windows (Vienna, Austria; https://www.R-project.org/).

3. Results

3.1. Arsenic cytotoxicity and metabolic dysregulations

To characterize the effects of As exposure on mature human adipocytes, we investigated the cytotoxic effects of As on AD-hMSCs after 48 h of exposure. Fig. 1A represents As cytotoxicity in AD-hMSCs with the inhibitory concentration 50 (IC50) calculated at 20 μM. We determined the IC10 and IC20 at 6 and 13 μM, respectively. Based on these results, we established an experimental range of concentrations between 10 nM and 10 μM, associated to a maximal 17% reduction of cell viability. In this interval of treatment concentrations, As intracellular levels were significantly increased from 1 μM in a dose-dependent manner, revealing the current absorption of As by cells (Fig. 1B).

To have a metabolic screening of the effects of As on AD-hMSCs, we performed untargeted metabolomics on cells treated with the four As concentrations for 48 h and detected a total of 12,339 metabolite features. The expression profile of the 150 most significantly impacted metabolite features across all the conditions of exposure clearly showed a dose-dependent effect of As on cells, with samples treated with As 1 μM and 10 μM forming two distinct clusters from control samples and samples treated with 10 and 100 nM of As (Fig. 1C). Among these 150 metabolite features, only 46 were identified and mainly correspond to lipid and fatty acid molecules (Supplementary Data 2). To go further and fully investigate the global metabolic impact of As on AD-hMSCs, we performed Linear Model for Micro Array Data (LIMMA) between controls and cells treated with 10 μM of As and highlighted 1577 significantly altered metabolite features. Importantly, the 150 dysregulated metabolite features previously revealed by one-way ANOVA were also the most significantly impacted in LIMMA analysis, bringing consistency to our results. Among the 1577 altered metabolic features, 357 were identified and the most significantly impacted were monoacylglycerols (MGs), diacylglycerols (DGs), triacylglycerols (TGs), ceramides, cholesteryl esters (CEs), phosphatidic acids (PAs), phosphatidylethanolamines (PEs), phosphatidylinositols (PIs), phosphatidylglycerols (PGs), phosphatidylserines (PSs), and essential fatty acids such as oleic acid, alpha-linolenic acid and palmitoleic acid. Strikingly, lipid and fatty acid molecules represent 84% of the identified metabolite features in As-treated AD-hMSCs, while the remaining 16% correspond to amino acids, nucleotides, sugars, vitamins and glutathione derivatives. The complete list of detected metabolite features is available in Supplementary Table 2. Over-representation pathway analysis revealed 253 biological pathways significantly altered by 10 μM As treatment (q-value < 0.01), whose first 30 are shown in Fig. 1D. In accordance with the identified metabolite features, we observed a strong effect on lipid (glycerophospholipid biosynthesis and phospholipid metabolism) and energy metabolism. In addition, we found that As dysregulated the transport of small molecules (SLC-mediated transmembrane transport and transport of vitamins, nucleosides and related molecules), signal transduction (GPCR downstream signaling) and immune system. The complete list of significantly dysregulated biological pathways is provided in Supplementary Table 3.

3.2. Dysregulation of lipid and energy homeostasis

Lipid storage and lipolysis are some of the main functions of white adipocytes to ensure energy homeostasis (Morigny et al., 2021). To understand how As dysregulates lipid metabolism, we investigated its impact on genes involved in fat storage and mobilization in AD-hMSCs. We measured the mRNA levels of Fatty Acid Synthase (FASN), Lipoprotein Lipase (LPL), Diacylglycerol O-Acyltransferase 2 (DGAT2), Lipin 1B and 2 (LPIN1B and LPIN2), Fatty Acid Binding Protein 4 (FABP4), Perilipin 1 (PLIN1), Patatin Like Phospholipase Domain Containing 2 (PNPLA2 or ATGL), Sterol Regulatory Element Binding Transcription Factor (SREBF1) and its predominant isoform SREBP1C after 48 h of As exposure. Overall, the expression of these genes was significantly decreased in a dose-dependent manner from 10 nM of As, except for FABP4, whose reduction was significant from 1 μM (Fig. 2A and Supplementary Data 1). These results were further associated with a significant decrease of lipid accumulation at 10 μM of As as revealed by Oil Red O staining (Fig. 2B and Supplementary Data 2). Besides impairing the ability of adipocytes to store lipids, As also reduced the expression of genes involved in adipogenesis and adipocyte functions such as the Peroxisome Proliferator Activated Receptor Gamma (PPARG), the Phosphoenolpyruvate Carboxykinase (PCK1), and the two adipokines Adiponectin (ADIPOQ) and Leptin (LEP), whose expression was significantly decreased in a dose-dependent manner, already from 10 nM of As (Fig. 2A and Supplementary Data 1).

Untargeted metabolomics also pinpointed the impact of As on multiple metabolite features, such as fructose 6-phosphate, glucose 6-phosphate, uridine diphosphate-N-acetylglucosamine, TGs, DGs and ceramides, associated to insulin resistance (q value = 7.96e-06, Supplementary Table 3). Insulin plays a key role in adipocytes by inhibiting lipolysis and triggering lipid storage and glucose uptake into the cells via the activation of a signaling cascade including the phosphorylation of Akt. To functionally assess if As impaired the ability of AD-hMSCs to respond to insulin, we measured Akt phosphorylation levels at the two highest As concentrations, 1 and 10 μM. As expected, we observed a significant increase of Akt phosphorylation upon insulin stimulation in control cells (Fig. 2C). At 10 μM of As, basal Akt phosphorylation was strongly dampened compared to controls and the response to insulin was impaired. These data suggested that As induced insulin resistance in mature adipocytes. In line with these observations, the mRNA levels of the Insulin Receptor Substrate 2 (IRS2) and the Glucose Transporter 4 (GLUT4), the insulin-sensitive glucose transporter in adipocytes, as well as the Pyruvate Kinase M1/2 (PKM2), involved in glycolysis, were significantly decreased, suggesting a strong impact of As on glucose homeostasis (Fig. 2A and Supplementary Data 1). Accordingly, we observed an effect of As on the biological pathways of carbohydrate metabolism, glucose metabolism, glycolysis and gluconeogenesis and the associated metabolites involved in these pathways. The concentrations of fructose-6-phosphate, glucose-6-phosphate, glycerol-3-phosphate obtained from glucose during glycolysis, malic acid and adenosine monophosphate were all significantly decreased by As treatment at 10 μM (Fig. 2D). In addition, the concentration of oxoglutaric acid was significantly increased at 10 μM.

Collectively, our data highlighted a massive dysregulation of lipid and glucose metabolism induced by arsenic exposure in adipocytes, associated with their reduced ability to store lipids and inhibited insulin sensitivity. Fig. 2E summarizes the impact of 10 μM of As on lipogenesis and glucose metabolism in mature adipocytes.

3.3. As homeostasis and cellular defense

Over-representation pathway analysis also revealed that As exposure significantly altered the transport of small molecules and inorganic ions (q value = 5.06e-18 and q value = 1.57e-3 respectively, Supplementary Table 3). In particular, glutathione is strongly involved in the metabolism and transport of As ions and glutathione metabolism was among

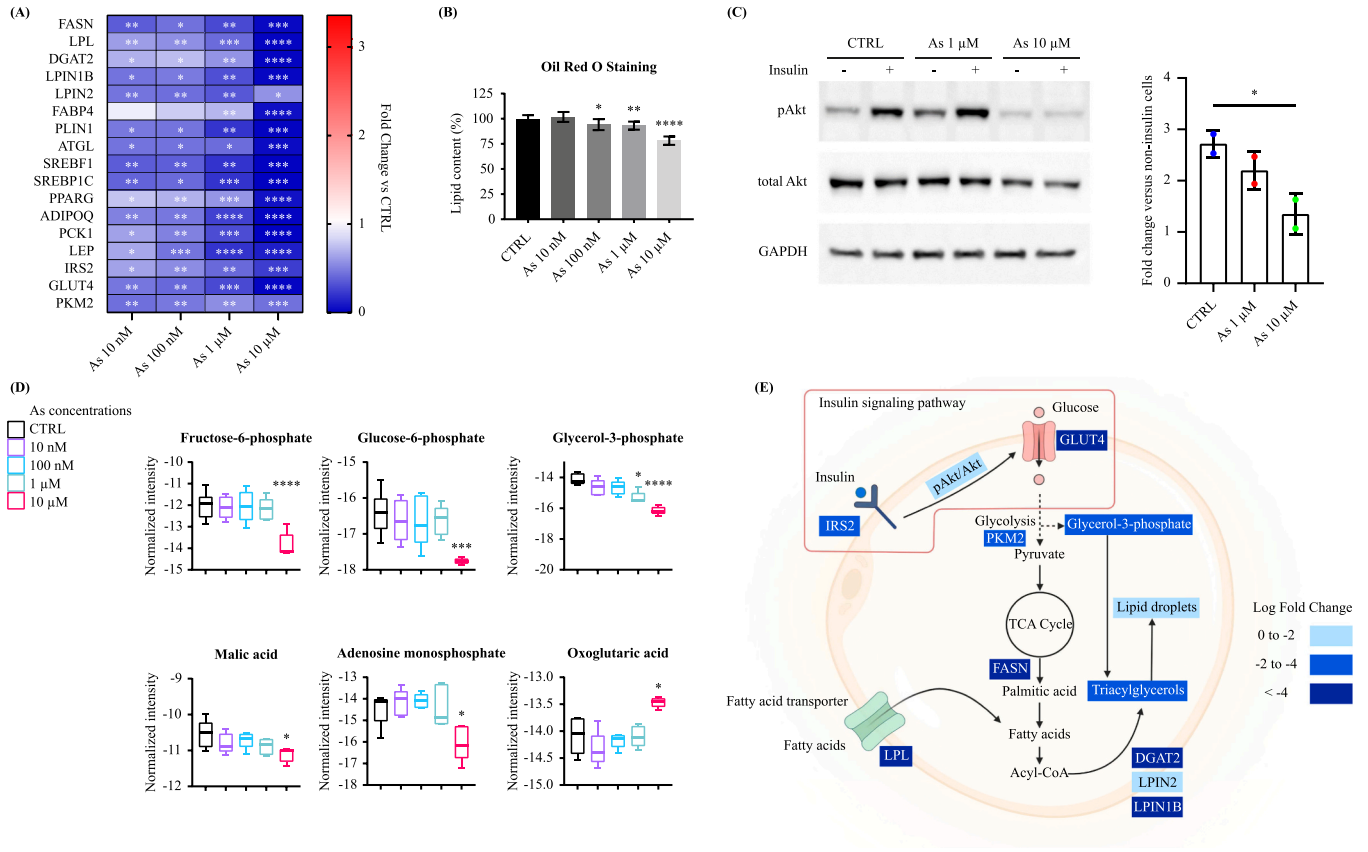

Fig. 2. Impact of arsenic exposure on lipogenesis. (A) Heatmap representation of the impact of arsenic exposure (10 nM to 10 µM, N = 5) during 48 h on genes involved in lipid metabolism, glucose metabolism and adipocyte functions. mRNA levels were normalized as a ratio to the corresponding RPS13 mRNA level. Relative expression and fold change were expressed between controls and arsenic-treated cells. (B) Quantification of the total lipid content of AD-hMSCs treated with arsenic (10 nM to 10 µM, N = 5 for controls, N = 7 for arsenic concentrations) during 48 h by Oil Red O Staining. (C) Western-blots of phosphorylated and total Akt in protein samples from AD-hMSCs treated with two arsenic concentrations, 1 and 10 µM, or control for 48 h, followed by 10 nM insulin stimulation for 15 min. GAPDH was used as an internal loading control. Protein expressions were quantified using ImageJ software. (D) Dysregulation of several metabolites involved in glucose homeostasis and carbohydrate metabolism during arsenic exposure (10 nM to 10 µM during 48 h, N = 5). (E) Impact of 10 µM of arsenic on lipogenesis and glucose metabolism in mature adipocytes. Dysregulated genes and metabolites are represented in blue as a log2 fold change versus controls. Error bars represent standard deviation. One-way ANOVA followed by Tukey or Dunnett post hoc test were used to analyze the differences between control and arsenic concentrations and * indicates significant changes versus controls (* $p < 0.05$, ** $p < 0.01$, *** $p < 0.001$, **** $p < 0.0001$).

the significantly affected metabolic pathways upon As exposure (q value = 6.07e-06, Supplementary Table 3), as demonstrated by increased levels of glutathione, glutathione disulfide, L-cysteinylglycine and γ-glutamylcysteine at the expenses of L-glutamate and 5-oxoproline, both significantly reduced (Fig. 3A and Supplementary Data 3). These changes reflected a strong induction of Glutamate-Cysteine Ligase Modifier Subunit (GCLM) gene that might explain the increased conversion of L-glutamate into γ-glutamylcysteine, further converted into glutathione (Ran et al., 2020), whereas Glutamate-Cysteine Ligase Catalytic Subunit (GCLC) and Glutathione Synthetase (GSS) were both slightly downregulated. The reduced expression of Gamma-Glutamylcyclotransferase (GGCT) and 5-Oxoprolinase, ATP-Hydrolysing (OPLAH), together with the decreased levels of 5-oxoproline and L-glutamate, suggests that glutathione was not degraded to replenish L-glutamate, but rather directed towards degradation into L-cysteinylglycine or oxidation into glutathione disulfide through Glutathione Peroxidase 4 (GPX4), hence participating in the maintenance of the red-ox cellular state. Interestingly, glutathione disulfide, the oxidized form of glutathione involved in the oxidation of reactive oxygen species, was significantly increased upon As treatment leading to a decreased ratio glutathione/glutathione disulfide, which is suggestive of the potential activation of an adaptive oxidative stress response.

As mentioned previously, the increase of glutathione production is highly relevant for As metabolism and detoxification in human adipocytes (Leslie, 2012). As ion influx and efflux in adipocytes is ensured by the glycerol bidirectional channel via Aquaporin 7 (AQP7) (Mukhopadhyay et al., 2014), whose expression was significantly decreased in a dose-dependent manner by As treatment. As ions conjugate with glutathione to favor their metabolism as tri-glutathione complexes ($As(GSH)_3$). Glutathione-S-Transferase Omega 1 (GSTO1) catalyzed this reaction, which was strongly increased at 10 µM of As. As $(GSH)_3$ complexes are further methylated by Arsenite Methyltransferase (AS3MT) to form monomethyl- and dimethyl-arsenic acids and their pentavalent forms, or directly extruded by the extrusion pump and the action of the two transporters ATP Binding Cassette Subfamily C Member 1 and 2 (MRP1/2). In our study, As treatment induced a mild but not significant decrease of AS3MT expression and As metabolites were not detected in cell and medium samples (data not shown). In parallel, we observed a mild significant decrease of MRP1 and MRP2 gene expressions, suggesting here again the potential accumulation of As within the cells.

Because of the significant accumulation of As and the possible activation of cellular stress, we investigated the impact of the treatment on the inflammatory response and the activation of the cell protection mechanisms. As shown in Fig. 3B, the mRNA levels of the cytokine C-C Motif Chemokine Ligand 2 (CCL2) significantly decreased in a dose-dependent manner, but 10 µM of As induced a significant increase of Interleukin 6 (IL6) expression, suggesting the activation of the pro-

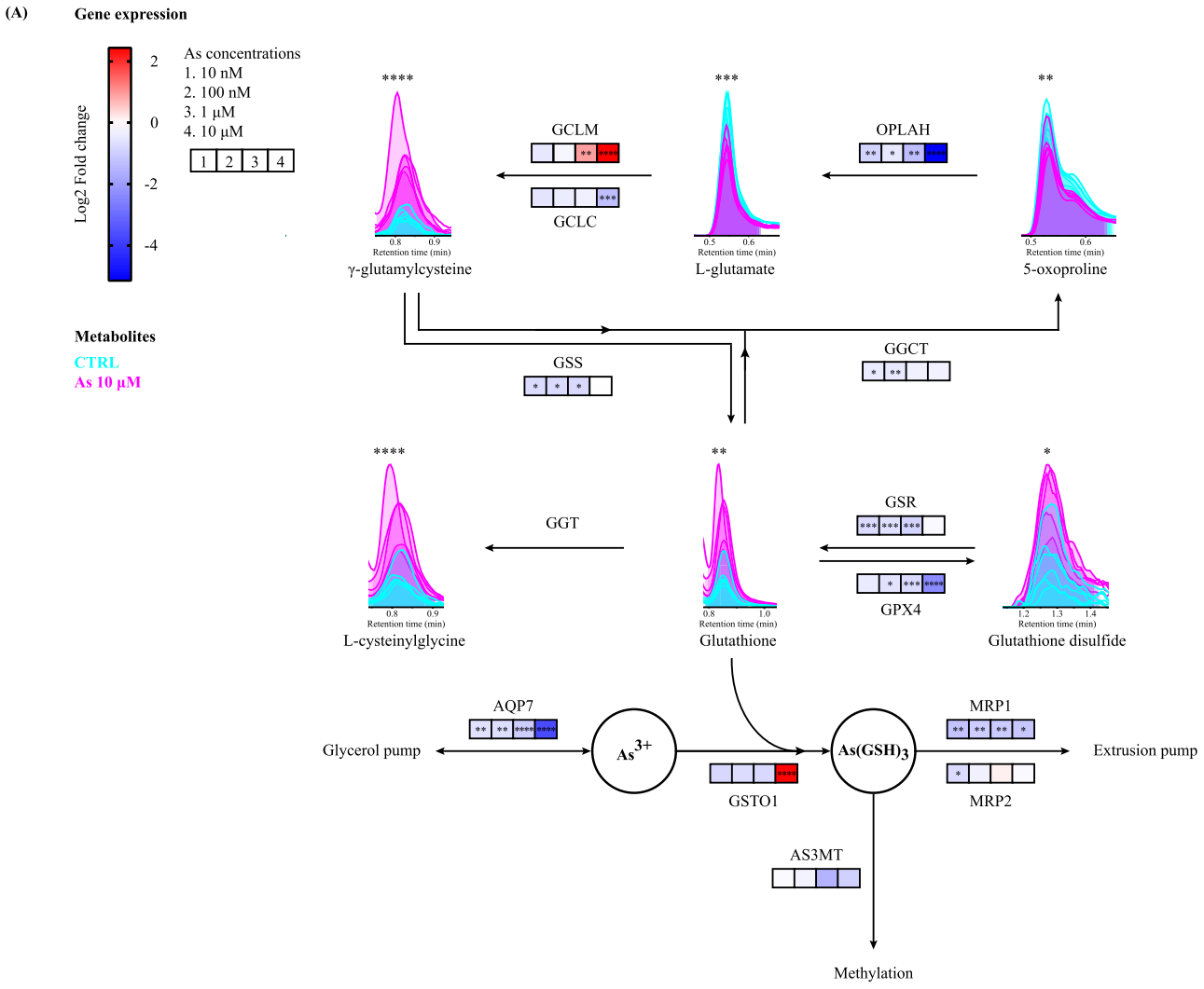

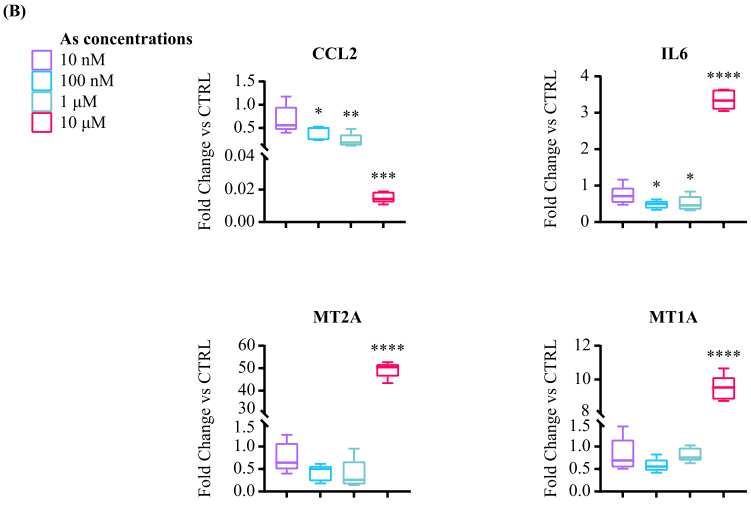

Fig. 3. Impact of arsenic on glutathione metabolism and adaptive oxidative stress response activation. (A) Representation of glutathione metabolism with significantly altered genes and metabolites after 48 h of exposure. Peak intensities represent the dysregulated metabolite features detected by untargeted metabolomics. Gene expressions are represented on the arrows in boxes with the associated reaction and are expressed as the log2 fold change between controls and arsenic-treated cells. (B) mRNA levels of CCL2, IL6, MT2A and MT1A after 48 h of arsenic exposure (10 nM to 10 µM, N = 5) were expressed as the relative expression and fold change between controls and arsenic-treated cells. Gene expressions were normalized as a ratio to the corresponding RPS13 mRNA level. One-way ANOVA followed by Tukey post hoc test were used to analyze the differences between controls and arsenic concentrations. The error bars represent standard deviation. For metabolites, statistical significance of differences in means from the control was calculated using LIMMA R package. (* $p < 0.05$, ** $p < 0.01$, *** $p < 0.001$, **** $p < 0.0001$).

inflammatory state of the adipocytes. We next checked the expression of two metallothionein (MT) isoforms, MT2A and MT1A, that belong to a class of cysteine-rich proteins involved in cell detoxification against heavy metal toxicity and the oxidative stress response. Both MT2A and MT1A were strongly induced by As exposure at 10 μM, supporting the activation of the adaptive oxidative stress response and defense mechanisms against As cytotoxicity. Collectively, our data showed that, despite the activation of these mechanisms, As exposure leads to the dysregulation of its homeostasis and transport and the development of inflammation in mature adipocytes.

4. Discussion

4.1. Arsenic concentrations and cytotoxicity

In our study, untargeted metabolomics was used as an unbiased approach to decipher the effects of an acute exposure to low As levels (from 10 nM to 10 μM) on mature human adipocytes. The World Health Organization (WHO) sets a recommended limit of exposure of 10 μg/L of As in drinking water (Brammer and Ravenscroft, 2009; UNICEF, 2018). So far, most of the *in vivo* studies exploring As metabolic effects used concentrations in drinking water between 100 μg/L and 50 mg/L, well beyond the WHO limit, which results in insulin resistance, impaired glucose tolerance and increased body weight (Calderon-DuPont et al., 2023; Paul et al., 2007b). However, it remains difficult to estimate the actual amount of As that reaches adipose tissue upon such exposure, and only one study determined that administration of 50 mg/L As for 8 weeks to mice would result in approximately 1 μM of As in adipose tissue (Paul et al., 2007b). *In vitro* studies exploring the direct effect of As in 3T3-L1 and AD-hMSCs span from 1 μM to 600 μM, which inhibit adipogenesis and insulin-stimulated glucose uptake, induce inflammation and oxidative stress (Garciafigueroa et al., 2013; Paul et al., 2007a; Walton et al., 2004). Our study covers a range of lower As doses, from 10 nM to 10 μM, perhaps more compatible with environmental exposure. At the highest concentration of 10 μM, the dysregulation of various metabolic pathways was associated with the induction of MTs and the increase of glutathione levels, while cell viability was reduced by only 17%. These results highlighted a strong metabolic perturbation and the potential activation of an adaptive oxidative stress response to counteract As toxicity. However, changes of the expression profile of genes involved in lipid and glutathione metabolism, As transport and adipocyte functions were already observed following an acute As exposure as low as 10 nM. In this view, it would be of great interest to investigate the metabolic consequences of a long-term exposure to these low concentration range on human adipocyte metabolism and assess systematically what are actual levels of As and its different species in adipose tissue in the general population.

4.2. Decreased insulin sensitivity and glucose handling

Within adipocytes, the action of insulin controls many cellular processes such as glucose uptake or lipid metabolism (Morigny et al., 2021). In our study, we demonstrated that As exposure downregulated IRS2 and GLUT4 levels and impaired the basal and insulin-stimulated Akt phosphorylation. These results suggest a strong inhibition of insulin signaling and ISGU, as also supported by the impact of As on various metabolite features involved in glucose metabolism. Our results are consistent with previous observations made in 3T3-L1 adipocytes at higher As concentrations and longer exposure durations (Paul et al., 2007a; Walton et al., 2004; Xue et al., 2011) and highlight the potential of As to induce insulin resistance in human adipocytes and impair cell ability to handle glucose. Interestingly, Xue and colleagues observed that, in 3T3-L1 adipocytes chronically exposed to As concentrations, the decreased insulin sensitivity and ISGU were associated with increased NRF2 activity, high intracellular levels of glutathione and inflammatory cytokines and decreased levels of several markers of adipocyte functions (Xue et al., 2011). Based on these results, authors hypothesized that the inhibition of ISGU could be promoted, at least in part, by the activation of the cellular oxidative stress response. In our study, we also observed a significant increase of glutathione levels and of the inflammatory cytokine IL6. This was associated with the inhibition of several key adipocyte genes such as PPARG, ADIPOQ, LEP and PCK1. Our results support the hypothesis of Xue and colleagues, although mechanistic experiments would be needed to demonstrate if a true causal link exists between the activation of an adaptive stress response and the development of insulin resistance in response to As exposure in human adipocytes.

4.3. Dysregulation of lipid metabolism

The development of insulin resistance in adipocytes might have a big impact on lipid metabolism. In adipocytes, triglyceride accumulation is controlled by the balance between lipogenesis and lipolysis. As mentioned previously, insulin is a key regulator of lipid metabolism which promotes the hydrolysis of circulating fatty acids via LPL before their uptake into cells via fatty acid transporters and their storage into adipocytes as TGs (Morigny et al., 2021). Insulin also activates SREBP1C which is involved in the regulation of several lipogenic genes, such as FASN and DGAT2 (Foretz et al., 1999). Finally, insulin is strongly involved in the inhibition of lipolysis in adipocytes. Accordingly, we found that, besides decreasing insulin sensitivity, As treatment reduced the expression of numerous genes involved in fatty acid metabolism and TG synthesis, suggesting an overall impairment of lipogenesis. This was further confirmed by the decreased cellular lipid content in response to As, the inhibition of PLIN1, involved in the regulation of lipid droplet size and a mandatory regulator of basal and stimulated lipolysis (Garciafigueroa et al., 2013), and of other markers of mature adipocytes such as PPARG, ADIPOQ, FABP4 and ATGL. In addition, despite the reduction of ATLG, involved in TG hydrolysis with adipocytes, our results pinpoint towards a potential functional deficit in lipid storage capacity and increased lipolysis, as also observed by Garciafigueroa and colleagues (Garciafigueroa et al., 2013). Interestingly, the loss of the adipose tissue ability to store lipids is strongly associated with the development of metabolic syndrome and oxidative stress (Vigouroux et al., 2011), because it potentially leads to ectopic lipid accumulation and the development of systemic inflammation (Gustafson et al., 2007; Turer et al., 2012). Collectively, given its strong ability to inhibit lipogenesis and lipid storage in human adipocytes, As would be an important risk factor for the development of T2D and metabolic syndrome.

4.4. Activation of the adaptive oxidative stress response

When As^{3+} ions enter the cells, they undergo several steps of metabolism. Liver is the main organ for As methylation prior excretion of the produced metabolites in kidneys (Chen et al., 2012). Less is known about As metabolism in adipose tissue, although one previous study showed evidence of poor As methylation capacity of adipocytes (Flora, 2011). In line with these observations, we did not detect any As metabolites and As treatment had no significant impact on AS3MT expression in AD-hMSCs, suggesting that As was not metabolized within the cells. Nevertheless, we demonstrated that As exposure activated several antioxidant molecules that could protect against As-induced toxicity. In particular, MTs and glutathione are thiol-rich molecules strongly involved in cell defense mechanisms and response to oxidative stress (Chiaverini and De Ley, 2010; Leslie, 2012). Trivalent arsenicals have high affinity for thiol groups and strongly bind to cysteine residues on proteins (Shen et al., 2013). In particular, each MT molecule can bind to six As ions (Jiang et al., 2003) leading to the formation of As-MT complexes (Ganger et al., 2016). In our study, we found that As exposure was able to significantly induce the expression levels of two MT isoforms, MT1A and MT2A. Glutathione also provides an important cellular protection against As toxicity with the formation of $As(GSH)_3$ complexes, which is promoted by GSTO1 (Patrick, 2003), a phase II enzyme

involved in xenobiotic detoxification (Chen et al., 2012), whose expression was strongly increased by As exposure in our experiments. Here, the overall increase of antioxidant levels in response to As toxicity suggests the activation of an adaptive oxidative stress response, as observed in other studies (Flora, 2011; Fu et al., 2010). In parallel, As significantly decreased the expression of GPX4, involved in the metabolism of reactive oxygen species (Flora, 2011). Interestingly, in *ob/ob* mice and 3T3-L1 mature adipocytes, decreased GPX activities and increased content of glutathione were associated with obesity and adipocyte dysfunction via the suppression of the insulin-induced tyrosine phosphorylation of IRS1, the subsequent interaction of PI3K to IRS1 and the serine phosphorylation of Akt (Kobayashi et al., 2009). Hence, glutathione accumulation and inhibition of GPX4 expression induced by As might participate to the development of insulin resistance in human adipocytes.

4.5. Arsenic metabolism and transport

Within adipocytes, As influx and efflux are ensured by different transporters such as MRPs and AQP7. MRPs are ATP-binding cassette transporters located in cell membrane (Watanabe and Hirano, 2013) and involved in the metabolism of xenobiotics and their metabolites (Leslie, 2012). MRP1 and MRP2 excrete As $As(GSH)_3$ into the circulation, the liver and the bile (Garbinski et al., 2019) hence conferring cellular protection against As cytotoxicity (Leslie, 2012). AQP7 is a bidirectional channel protein involved in the movement of As in and out of human cells (Mukhopadhyay et al., 2014) and, it is also the primary glycerol transporter in human adipose tissue (González-Dávalos et al., 2020). Altogether, the combined downregulation of AQP7 and MRP transporters observed in our study suggests that As exposure might have an impact on cell detoxification capacity, even at the lowest concentration investigated herein (10 nM), thus potentially exacerbating As accumulation and toxicity into cells. In addition, given its involvement in glycerol release from the adipocytes into the bloodstream (Leslie, 2012; Garbinski et al., 2019) AQP7 is also thought to play an important role in adipose tissue enlargement and adipocyte function (Garbinski et al., 2019). Accordingly, reduced AQP7 mRNA expression has been detected in obese men and women in several studies (Marrades et al., 2006; Ceperuelo-Mallafre et al., 2007) and AQP7 reduction in response to As might also contribute to deteriorate adipocyte metabolic functions.

5. Conclusion

We demonstrated that acute As exposure induces various metabolic perturbations in mature human adipocytes that might contribute to the development of T2D and metabolic syndrome. In particular, we highlighted that, despite the activation of cellular defense mechanisms, with the induction of MTs and glutathione, As reduces adipocyte ability to store lipids, likely via the perturbation of insulin signaling and dysregulated glucose metabolism. Moreover, the downregulation of transporters involved in As metabolism could possibly participate to As toxicity. Our study gives robust mechanistic bases to understand As implication in the development of metabolic diseases in humans. The significant effects of As on mature adipocytes, observed here after a short period of exposure, raise the question of the possible consequences of chronic environmental exposure on adipose tissue homeostasis in the general population.

CRediT authorship contribution statement

Marie Gasser: Conceptualization, Methodology, Software, Validation, Formal analysis, Investigation, Data curation, Writing – original draft, Visualization. **Sébastien Lenglet**: Resources, Investigation, Writing – review & editing. **Nasim Bararpour**: Software, Resources, Formal analysis, Writing – review & editing. **Tatjana Sajic**: Formal analysis, Writing – review & editing. **Julien Vaucher**: Resources, Funding acquisition, Writing – review & editing. **Kim Wiskott**: Resources, Writing – review & editing. **Marc Augsburger**: Resources, Writing – review & editing. **Tony Fracasso**: Project administration, Funding acquisition, Writing – review & editing. **Federica Gilardi**: Conceptualization, Methodology, Visualization, Project administration, Supervision, Funding acquisition, Writing – original draft, Writing – review & editing. **Aurélien Thomas**: Conceptualization, Visualization, Supervision, Project administration, Funding acquisition, Writing – review & editing.

Declaration of Competing Interest

The authors declare that they have no known competing financial interests or personal relationships that could have appeared to influence the work reported in this paper.

Data Availability

Metabolomic data are available in Metabolights database with the following ID: MTBLS8808 (www.ebi.ac.uk/metabolights/MTBLS8808).

Acknowledgment

This research was supported by Swiss National Science Foundation [grant #31003A-182420] to AT and TF and the Prix de la Fondation pour la Recherche sur le Diabète 2020 to AT and JV.

Appendix A. Supporting information

Supplementary data associated with this article can be found in the online version at doi:10.1016/j.tox.2023.153672.

References

Afridi, H.I., Kazi, T.G., Kazi, N., Jamali, M.K., Arain, M.B., Jalbani, N., Baig, J.A., Sarfraz, R.A., 2008. Evaluation of status of toxic metals in biological samples of diabetes mellitus patients. Diabetes Res Clin. Pr. 80, 280–288. https://doi.org/10.1016/j.diabres.2007.12.021.

Ahangarpour, A., Alboghobeish, S., Rezaei, M., Khodayar, M.J., Oroojan, A.A., Zainvand, M., 2018. Evaluation of diabetogenic mechanism of high fat diet in combination with arsenic exposure in male mice. Iran. J. Pharm. Res. 17, 164–183.

Bararpour, N., Gilardi, F., Carmeli, C., Sidibe, J., Ivanisevic, J., Caputo, T., Augsburger, M., Grabherr, S., Desvergne, B., Guex, N., Bochud, M., Thomas, A., 2021. DBnorm as an R package for the comparison and selection of appropriate statistical methods for batch effect correction in metabolomic studies. Sci. Rep. 11, 5657. https://doi.org/10.1038/s41598-021-84824-3.

Barber, R.D., Harmer, D.W., Coleman, R.A., Clark, B.J., 2005. GAPDH as a housekeeping gene: analysis of GAPDH mRNA expression in a panel of 72 human tissues. Physiol. Genom. 21, 389–395. https://doi.org/10.1152/physiolgenomics.00025.2005.

Brammer, H., Ravenscroft, P., 2009. Arsenic in groundwater: a threat to sustainable agriculture in South and South-east Asia. Environ. Int 35, 647–654. https://doi.org/10.1016/j.envint.2008.10.004.

Calderon-DuPont, D., Romero-Cordoba, S.L., Tello, J.K., Espinosa, A., Guerrero, B., Contreras, A.V., Moran-Ramos, S., Diaz-Villasenor, A., 2023. Impaired white adipose tissue fatty acid metabolism in mice fed a high-fat diet worsened by arsenic exposure, primarily affecting retroperitoneal adipose tissue. Toxicol. Appl. Pharm. 468, 116428 https://doi.org/10.1016/j.taap.2023.116428.

Castriota, F., Acevedo, J., Ferreccio, C., Smith, A.H., Liaw, J., Smith, M.T., Steinmaus, C., 2018. Obesity and increased susceptibility to arsenic-related type 2 diabetes in Northern Chile. Environ. Res 167, 248–254. https://doi.org/10.1016/j.envres.2018.07.022.

Ceja-Galicia, Z.A., Daniel, A., Salazar, A.M., Panico, P., Ostrosky-Wegman, P., Diaz-Villasenor, A., 2017. Effects of arsenic on adipocyte metabolism: Is arsenic an obesogen? Mol. Cell Endocrinol. 452, 25–32. https://doi.org/10.1016/j.mce.2017.05.008.

Ceperuelo-Mallafre, V., Miranda, M., Chacon, M.R., Vilarrasa, N., Megia, A., Gutierrez, C., Fernandez-Real, J.M., Gomez, J.M., Caubet, E., Fruhbeck, G., Vendrell, J., 2007. Adipose tissue expression of the glycerol channel aquaporin-7 gene is altered in severe obesity but not in type 2 diabetes. J. Clin. Endocrinol. Metab. 92, 3640–3645. https://doi.org/10.1210/jc.2007-0531.

Chambers, M.C., Maclean, B., Burke, R., Amodei, D., Ruderman, D.L., Neumann, S., Gatto, L., Fischer, B., Pratt, B., Egertson, J., Hoff, K., Kessner, D., Tasman, N., Shulman, N., Frewen, B., Baker, T.A., Brusniak, M.Y., Paulse, C., Creasy, D., Flashner, L., Kani, K., Moulding, C., Seymour, S.L., Nuwaysir, L.M., Lefebvre, B., Kuhlmann, F., Roark, J., Rainer, P., Detlev, S., Hemenway, T., Huhmer, A., Langridge, J., Connolly, B., Chadick, T., Holly, K., Eckels, J., Deutsch, E.W.,

Moritz, R.L., Katz, J.E., Agus, D.B., MacCoss, M., Tabb, D.L., Mallick, P., 2012. A cross-platform toolkit for mass spectrometry and proteomics. Nat. Biotechnol. 30, 918–920. https://doi.org/10.1038/nbt.2377.
Chen, J.W., Wang, S.L., Wang, Y.H., Sun, C.W., Huang, Y.L., Chen, C.J., Li, W.F., 2012. Arsenic methylation, GSTO1 polymorphisms, and metabolic syndrome in an arseniasis endemic area of southwestern Taiwan. Chemosphere 88, 432–438. https://doi.org/10.1016/j.chemosphere.2012.02.059.
Chen, Y.W., Yang, C.Y., Huang, C.F., Hung, D.Z., Leung, Y.M., Liu, S.H., 2009. Heavy metals, islet function and diabetes development. Islets 1, 169–176. https://doi.org/10.4161/isl.1.3.9262.
Cheng, H., Qiu, L., Zhang, H., Cheng, M., Li, W., Zhao, X., Liu, K., Lei, L., Ma, J., 2011. Arsenic trioxide promotes senescence and regulates the balance of adipogenic and osteogenic differentiation in human mesenchymal stem cells. Acta Biochim Biophys. Sin. 43, 204–209. https://doi.org/10.1093/abbs/gmq130.
Chiaverini, N., De Ley, M., 2010. Protective effect of metallothionein on oxidative stress-induced DNA damage. Free Radic. Res 44, 605–613. https://doi.org/10.3109/10715761003692511.
Coelho, P., Costa, S., Costa, C., Silva, S., Walter, A., Ranville, J., Pastorinho, M.R., Harrington, C., Taylor, A., Dall'Armi, V., Zoffoli, R., Candeias, C., da Silva, E.F., Bonassi, S., Laffon, B., Teixeira, J.P., 2014. Biomonitoring of several toxic metal (loid)s in different biological matrices from environmentally and occupationally exposed populations from Panasqueira mine area, Portugal. Environ. Geochem. Health 36, 255–269. https://doi.org/10.1007/s10653-013-9562-7.
Diaz-Villasenor, A., Burns, A.L., Hiriart, M., Cebrian, M.E., Ostrosky-Wegman, P., 2007. Arsenic-induced alteration in the expression of genes related to type 2 diabetes mellitus. Toxicol. Appl. Pharm. 225, 123–133. https://doi.org/10.1016/j.taap.2007.08.019.
Drobna, Z., Walton, F.S., Paul, D.S., Xing, W., Thomas, D.J., Styblo, M., 2010. Metabolism of arsenic in human liver: the role of membrane transporters. Arch. Toxicol. 84, 3–16. https://doi.org/10.1007/s00204-009-0499-7.
Ettinger, A.S., Zota, A.R., Amarasiriwardena, C.J., Hopkins, M.R., Schwartz, J., Hu, H., Wright, R.O., 2009. Maternal arsenic exposure and impaired glucose tolerance during pregnancy. Environ. Health Perspect. 117, 1059–1064. https://doi.org/10.1289/ehp0800533.
Farkhondeh, T., Samarghandian, S., Azimi-Nezhad, M., 2019. The role of arsenic in obesity and diabetes. J. Cell Physiol. 234, 12516–12529. https://doi.org/10.1002/jcp.28112.
Farzan, S.F., Howe, C.G., Zens, M.S., Palys, T., Channon, J.Y., Li, Z., Chen, Y., Karagas, M. R., 2017. Urine arsenic and arsenic metabolites in U.S. adults and biomarkers of inflammation, oxidative stress, and endothelial dysfunction: a cross-sectional study. Environ. Health Perspect. 125, 127002 https://doi.org/10.1289/EHP2062.
Flora, S.J., 2011. Arsenic-induced oxidative stress and its reversibility. Free Radic. Biol. Med. 51, 257–281. https://doi.org/10.1016/j.freeradbiomed.2011.04.008.
Foretz, M., Guichard, C., Ferré, P., Foufelle, F., 1999. Sterol regulatory element binding protein-1c is a major mediator of insulin action on the hepatic expression of glucokinase and lipogenesis-related genes. PNAS 96, 12737–12742.
Freire, C., Vrhovnik, P., Fiket, Z., Salcedo-Bellido, I., Echeverria, R., Martin-Olmedo, P., Kniewald, G., Fernandez, M.F., Arrebola, J.P., 2020. Adipose tissue concentrations of arsenic, nickel, lead, tin, and titanium in adults from GraMo cohort in Southern Spain: An exploratory study. Sci. Total Environ. 719, 137458 https://doi.org/10.1016/j.scitotenv.2020.137458.
Fu, J., Woods, C.G., Yehuda-Shnaidman, E., Zhang, Q., Wong, V., Collins, S., Sun, G., Andersen, M.E., Pi, J., 2010. Low-level arsenic impairs glucose-stimulated insulin secretion in pancreatic beta cells: involvement of cellular adaptive response to oxidative stress. Environ. Health Perspect. 118, 864–870. https://doi.org/10.1289/ehp.0901608.
Ganger, R., Garla, R., Mohanty, B.P., Bansal, M.P., Garg, M.L., 2016. Protective effects of zinc against acute arsenic toxicity by regulating antioxidant defense system and cumulative metallothionein expression. Biol. Trace Elem. Res 169, 218–229. https://doi.org/10.1007/s12011-015-0400-x.
Garbinski, L.D., Rosen, B.P., Chen, J., 2019. Pathways of arsenic uptake and efflux. Environ. Int 126, 585–597. https://doi.org/10.1016/j.envint.2019.02.058.
Garciafigueroa, D.Y., Klei, L.R., Ambrosio, F., Barchowsky, A., 2013. Arsenic-stimulated lipolysis and adipose remodeling is mediated by G-protein-coupled receptors. Toxicol. Sci. 134, 335–344. https://doi.org/10.1093/toxsci/kft108.
Gasser, M., Lenglet, S., Bararpour, N., Sajic, T., Wiskott, K., Augsburger, M., Fracasso, T., Gilardi, F., Thomas, A., 2022. Cadmium acute exposure induces metabolic and transcriptomic perturbations in human mature adipocytes. Toxicology 470, 153153. https://doi.org/10.1016/j.tox.2022.153153.
González-Dávalos, L., Álvarez-Pérez, M., Quesada-López, T., Cereijo, R., Campderrós, L., Piña, E., Shimada, A., Villarroya, F., Varela-Echavarria, A., Mora, O., 2020. Chapter nine - glucocorticoid gene regulation of aquaporin-7. Vitam. Horm. 112, 179–207. https://doi.org/10.1016/bs.vh.2019.08.005.
Gorzelniak, K., Janke, J., Engeli, S., Sharma, A.M., 2001. Validation of endogenous controls for gene expression studies in human adipocytes and preadipocytes. Horm. Metab. Res 33, 625–627. https://doi.org/10.1055/s-2001-17911.
Grau-Perez, M., Kuo, C.C., Gribble, M.O., Balakrishnan, P., Jones Spratlen, M., Vaidya, D., Francesconi, K.A., Goessler, W., Guallar, E., Silbergeld, E.K., Umans, J.G., Best, L.G., Lee, E.T., Howard, B.V., Cole, S.A., Navas-Acien, A., 2017. Association of low-moderate arsenic exposure and arsenic metabolism with incident diabetes and insulin resistance in the strong heart family study. Environ. Health Perspect. 125, 127004 https://doi.org/10.1289/EHP2566.
Gribble, M.O., Howard, B.V., Umans, J.G., Shara, N.M., Francesconi, K.A., Goessler, W., Crainiceanu, C.M., Silbergeld, E.K., Guallar, E., Navas-Acien, A., 2012. Arsenic exposure, diabetes prevalence, and diabetes control in the strong heart study. Am. J. Epidemiol. 176, 865–874. https://doi.org/10.1093/aje/kws153.
Gustafson, B., Hammarstedt, A., Andersson, C.X., Smith, U., 2007. Inflamed adipose tissue: a culprit underlying the metabolic syndrome and atherosclerosis. Arterioscler. Thromb. Vasc. Biol. 27, 2276–2283. https://doi.org/10.1161/ATVBAHA.107.147835.
Islam, R., Khan, I., Hassan, S.N., McEvoy, M., D'Este, C., Attia, J., Peel, R., Sultana, M., Akter, S., Milton, A.H., 2012. Association between type 2 diabetes and chronic arsenic exposure in drinking water: a cross sectional study in Bangladesh. Environ. Health 11, 38. https://doi.org/10.1186/1476-069X-11-38.
Jiang, G., Gong, Z., Li, X.F., Cullen, W.R., Chris Le, X., 2003. Interaction of trivalent arsenicals with metallothionein. Chem. Res. Toxicol. 16, 873–880.
Jomova, K., Jenisova, Z., Feszterova, M., Baros, S., Liska, J., Hudecova, D., Rhodes, C.J., Valko, M., 2011. Arsenic: toxicity, oxidative stress and human disease. J. Appl. Toxicol. 31, 95–107. https://doi.org/10.1002/jat.1649.
Kirkley, A.G., Carmean, C.M., Ruiz, D., Ye, H., Regnier, S.M., Poudel, A., Hara, M., Kamau, W., Johnson, D.N., Roberts, A.A., Parsons, P.J., Seino, S., Sargis, R.M., 2018. Arsenic exposure induces glucose intolerance and alters global energy metabolism. Am. J. Physiol. Regul. Integr. Comp. Physiol. 314, R294–R303. https://doi.org/10.1152/ajpregu.00522.2016.
Klei, L.R., Garciafigueroa, D.Y., Barchowsky, A., 2013. Arsenic activates endothelin-1 Gi protein-coupled receptor signaling to inhibit stem cell differentiation in adipogenesis. Toxicol. Sci. 131, 512–520. https://doi.org/10.1093/toxsci/kfs323.
Kobayashi, H., Matsuda, M., Fukuhara, A., Komuro, R., Shimomura, I., 2009. Dysregulated glutathione metabolism links to impaired insulin action in adipocytes. Am. J. Physiol. Endocrinol. Metab. 296, E1326–E1334. https://doi.org/10.1152/ajpendo.90921.2008.
Kuo, C.C., Moon, K.A., Wang, S.L., Silbergeld, E., Navas-Acien, A., 2017. The association of arsenic metabolism with cancer, cardiovascular disease, and diabetes: a systematic review of the epidemiological evidence. Environ. Health Perspect. 125, 087001 https://doi.org/10.1289/EHP577.
Lai, M.S., Hsueh, Y.M., CHen, C.J., Shyu, M.P., Chen, S.Y., Kuo, T.L., Wu, M.M., Tai, T.Y., 1993. Ingested inorganic arsenic and prevalence of diabetes mellitus. Am. J. Epidemiol. 135.
Leslie, E.M., 2012. Arsenic-glutathione conjugate transport by the human multidrug resistance proteins (MRPs/ABCCs). J. Inorg. Biochem 108, 141–149. https://doi.org/10.1016/j.jinorgbio.2011.11.009.
Marrades, M.P., Milagro, F.I., Martinez, J.A., Moreno-Aliaga, M.J., 2006. Differential expression of aquaporin 7 in adipose tissue of lean and obese high fat consumers. Biochem Biophys. Res Commun. 339, 785–789. https://doi.org/10.1016/j.bbrc.2005.11.080.
Matthae, S., May, S., Hubersberger, M., Hauner, H., Skurk, T., 2013. Protein normalization in different adipocyte models and dependence on cell size. Horm. Metab. Res 45, 572–580. https://doi.org/10.1055/s-0033-1341429.
Morigny, P., Boucher, J., Arner, P., Langin, D., 2021. Lipid and glucose metabolism in white adipocytes: pathways, dysfunction and therapeutics. Nat. Rev. Endocrinol. 17, 276–295. https://doi.org/10.1038/s41574-021-00471-8.
Mukhopadhyay, R., Bhattacharjee, H., Rosen, B.P., 2014. Aquaglyceroporins: generalized metalloid channels. Biochim Biophys. Acta 1840, 1583–1591. https://doi.org/10.1016/j.bbagen.2013.11.021.
Ochoa-Martinez, A.C., Ruiz-Vera, T., Almendarez-Reyna, C.I., Zarazua, S., Carrizales-Yanez, L., Perez-Maldonado, I.N., 2019. Impact of arsenic exposure on clinical biomarkers indicative of cardiovascular disease risk in Mexican women. Ecotoxicol. Environ. Saf. 169, 678–686. https://doi.org/10.1016/j.ecoenv.2018.11.088.
Padmaja Divya, S., Pratheeshkumar, P., Son, Y.O., Vinod Roy, R., Andrew Hitron, J., Kim, D., Dai, J., Wang, L., Asha, P., Huang, B., Xu, M., Luo, J., Zhang, Z., 2015. Arsenic induces insulin resistance in mouse adipocytes and myotubes via oxidative stress-regulated mitochondrial Sirt3-FOXO3a signaling pathway. Toxicol. Sci. 146, 290–300. https://doi.org/10.1093/toxsci/kfv089.
Palacios, J., Roman, D., Cifuentes, F., 2012. Exposure to low level of arsenic and lead in drinking water from Antofagasta city induces gender differences in glucose homeostasis in rats. Biol. Trace Elem. Res. 148, 224–231. https://doi.org/10.1007/s12011-012-9355-3.
Patrick, L., 2003. Toxic metals and antioxidants: Part II. The role of antioxidants in arsenic and cadmium toxicity. Altern. Med. Rev. 8, 106–128.
Paul, D.S., Devesa, V., Hernandez-Zavala, A., Adair, B.M., Walton, F.S., Drobna, Z., Thomas, D.J., Styblo, M., 2008. Environmental arsenic as a disruptor of insulin signaling. Met Ions Biol. Med. 10, 1–7.
Paul, D.S., Harmon, A.W., Devesa, V., Thomas, D.J., Styblo, M., 2007. Molecular mechanisms of the diabetogenic effects of arsenic: inhibition of insulin signaling by arsenite and methylarsonous acid. Environ. Health Perspect. 115, 734–742. https://doi.org/10.1289/ehp.9867.
Paul, D.S., Hernandez-Zavala, A., Walton, F.S., Adair, B.M., Dedina, J., Matousek, T., Styblo, M., 2007. Examination of the effects of arsenic on glucose homeostasis in cell culture and animal studies: development of a mouse model for arsenic-induced diabetes. Toxicol. Appl. Pharm. 222, 305–314. https://doi.org/10.1016/j.taap.2007.01.010.
Perrais, M., A. Thomas, M. Augsburger, S. Lenglet. 2023. Comparison of Dried Blood Spot and Microtube Techniquesfor Trace Element Quantification by ICP-MS, J Anal Toxicol, 47: 175–81. https://doi.org/10.1093/jat/bkad019.
Qin, Yan Yan, Clement Kai Man Leung, Anna Oi. Wah Leung, Sheng Chun Wu, Jin Shu Zheng, Ming Hung, Wong, 2009. Persistent organic pollutants and heavy metals in adipose tissues of patients with uterine leiomyomas and the association of these pollutants with seafood diet, BMI, and age. Environ. Sci. Pollut. Res. 17, 229–240. https://doi.org/10.1007/s11356-009-0251-0.
Rahman, M.M., Ng, J.C., Naidu, R., 2009. Chronic exposure of arsenic via drinking water and its adverse health impacts on humans. Environ. Geochem Health 31 (Suppl 1), 189–200. https://doi.org/10.1007/s10653-008-9235-0.

Rahman, M., Tondel, M., Ahmad, S.A., Axelson, O., 1998. Diabetes mellitus associated with arsenic exposure in Bangladesh. Am. J. Epidemiol. 148.
Ran, S., Liu, J., Li, S., 2020. A systematic review of the various effect of arsenic on glutathione synthesis in vitro and in vivo. Biomed. Res. Int. 2020, 9414196. https://doi.org/10.1155/2020/9414196.
Rhee, S.Y., Hwang, Y.C., Woo, J.T., Chin, S.O., Chon, S., Kim, Y.S., 2013. Arsenic exposure and prevalence of diabetes mellitus in Korean adults. J. Korean Med Sci. 28, 861–868. https://doi.org/10.3346/jkms.2013.28.6.861.
Ritchie, M.E., Phipson, B., Wu, D., Hu, Y., Law, C.W., Shi, W., Smyth, G.K., 2015. limma powers differential expression analyses for RNA-sequencing and microarray studies. Nucleic Acids Res 43, e47. https://doi.org/10.1093/nar/gkv007.
Shen, S., Li, X.F., Cullen, W.R., Weinfeld, M., Le, X.C., 2013. Arsenic binding to proteins. Chem. Rev. 113, 7769–7792. https://doi.org/10.1021/cr300015c.
Turer, A.T., Hill, J.A., Elmquist, J.K., Scherer, P.E., 2012. Adipose tissue biology and cardiomyopathy: translational implications. Circ. Res 111, 1565–1577. https://doi.org/10.1161/CIRCRESAHA.111.262493.
UNICEF. 2018. Arsenic primer: Guidance on the investigation and mitigation of arsenic contamination.
Vigouroux, C., Caron-Debarle, M., Le Dour, C., Magre, J., Capeau, J., 2011. Molecular mechanisms of human lipodystrophies: from adipocyte lipid droplet to oxidative stress and lipotoxicity. Int J. Biochem Cell Biol. 43, 862–876. https://doi.org/10.1016/j.biocel.2011.03.002.
Walton, F.S., Harmon, A.W., Paul, D.S., Drobna, Z., Patel, Y.M., Styblo, M., 2004. Inhibition of insulin-dependent glucose uptake by trivalent arsenicals: possible mechanism of arsenic-induced diabetes. Toxicol. Appl. Pharm. 198, 424–433. https://doi.org/10.1016/j.taap.2003.10.026.
Wang, Z.X., Jiang, C.S., Wang, X.H., Jin, H.J., Wu, Q., Chen, Q., 2005. The role of Akt on arsenic trioxide suppression of 3T3-L1 preadipocyte differentiation. Cell Res. 15 (5), 379–386.
Watanabe, T., Hirano, S., 2013. Metabolism of arsenic and its toxicological relevance. Arch. Toxicol. 87, 969–979. https://doi.org/10.1007/s00204-012-0904-5.
Xue, P., Hou, Y., Zhang, Q., Woods, C.G., Yarborough, K., Liu, H., Sun, G., Andersen, M. E., Pi, J., 2011. Prolonged inorganic arsenite exposure suppresses insulin-stimulated AKT S473 phosphorylation and glucose uptake in 3T3-L1 adipocytes: involvement of the adaptive antioxidant response. Biochem Biophys. Res. Commun. 407, 360–365. https://doi.org/10.1016/j.bbrc.2011.03.024.
Yadav, S., Anbalagan, M., Shi, Y., Wang, F., Wang, H., 2013. Arsenic inhibits the adipogenic differentiation of mesenchymal stem cells by down-regulating peroxisome proliferator-activated receptor gamma and CCAAT enhancer-binding proteins. Toxicol. Vitr. 27, 211–219. https://doi.org/10.1016/j.tiv.2012.10.012.
Yang, Q., Wang, Y., Zhang, Y., Li, F., Xia, W., Zhou, Y., Qiu, Y., Li, H., Zhu, F., 2020. NOREVA: enhanced normalization and evaluation of time-course and multi-class metabolomic data. Nucleic Acids Res. 48, W436–W448. https://doi.org/10.1093/nar/gkaa258.